Published in final edited form as:
Curr Neurovasc Res. 2011 August 1; 8(3): 220–235.

Erythropoietin Employs Cell Longevity Pathways of SIRT1 to Foster Endothelial Vascular Integrity During Oxidant Stress

Jinling Hou[1,2], **Shaohui Wang**[1,2], **Yan Chen Shang**[1,2], **Zhao Zhong Chong**[1,2], and **Kenneth Maiese**[*,1,2]

[1]Department of Neurology and Neurosciences, University of Medicine and Dentistry, New Jersey Medical School, Newark, New Jersey 07101, USA

[2]Cancer Center, New Jersey Medical School, University of Medicine and Dentistry, New Jersey Medical School, Newark, New Jersey 07101, USA

Abstract

Given the cytoprotective ability of erythropoietin (EPO) in cerebral microvascular endothelial cells (ECs) and the invaluable role of ECs in the central nervous system, it is imperative to elucidate the cellular pathways for EPO to protect ECs against brain injury. Here we illustrate that EPO relies upon the modulation of SIRT1 (silent mating type information regulator 2 homolog 1) in cerebral microvascular ECs to foster cytoprotection during oxygen-glucose deprivation (OGD). SIRT1 activation which results in the inhibition of apoptotic early membrane phosphatidylserine (PS) externalization and subsequent DNA degradation during OGD becomes a necessary component for EPO protection in ECs, since inhibition of SIRT1 activity or diminishing its expression by gene silencing abrogates cell survival supported by EPO during OGD. Furthermore, EPO promotes the subcellular trafficking of SIRT1 to the nucleus which is necessary for EPO to foster vascular protection. EPO through SIRT1 averts apoptosis through activation of protein kinase B (Akt1) and the phosphorylation and cytoplasmic retention of the forkhead transcription factor FoxO3a. SIRT1 through EPO activation also utilizes mitochondrial pathways to prevent mitochondrial depolarization, cytochrome c release, and Bad, caspase 1, and caspase 3 activation. Our work identifies novel pathways for EPO in the vascular system that can govern the activity of SIRT1 to prevent apoptotic injury through Akt1, FoxO3a phosphorylation and trafficking, mitochondrial membrane permeability, Bad activation, and caspase 1 and 3 activities in ECs during oxidant stress.

Keywords

Akt; apoptosis; Bad; caspase; endothelial; erythropoietin; FoxO3a; mitochondria; phosphatidylserine; sirtuin

INTRODUCTION

Interest for the role and biological activity of erythropoietin (EPO) in systems exclusive of the hematopoietic system continues at an astounding rate, especially in vascular and neuronal pathways [1-11]. EPO may be protective for a number of disorders such as diabetes [6, 12-17], atherosclerosis [18], angiogenesis [19-22], neurodegenerative disorders [23-26],

[*]Address correspondence to this author at the Department of Neurology and Neurosciences, Cancer Center, F1220, UMDNJ – New Jersey Medical School, 205 South Orange Avenue, Newark, NJ 0710, USA; wntin75@yahoo.com .

and ischemic injury [2, 5, 24, 27-31]. For the vascular system with endothelial cells (ECs), several cellular signals can serve as essential components for EPO to protect ECs, such as the serine/threonine kinase protein kinase B (Akt) [2, 5, 32-35], the signal transducer and activator of transcription (STAT) [5, 20, 36, 37], caspases [3, 12, 38], and the Bad, Bcl-x_L/Bcl-2 pathway [4, 39].

EPO also appears to govern the forkhead transcription factor FoxO3a which is linked to pathways of cell death, metabolism, and longevity [5, 12, 40-44]. As a downstream target of Akt, FoxO3a through EPO can be phosphorylated and retained in the cytoplasm preventing nuclear translocation and apoptotic injury [5]. Interestingly, the sirtuin (silent mating type information regulation 2 homolog) 1 (S. cerevisiae) (SIRT1) can deacetylate histones and transcription factors [45-50] including FoxO3a to control cellular survival [51, 52].

Given the relationship among EPO, Akt1, FoxO3a, and potentially SIRT1, we investigated the ability of EPO to modulate SIRT1 expression, activity, and cellular trafficking. We demonstrate in an oxidant stress oxygen-glucose deprivation model that EPO increases endogenous SIRT1 activity in ECs and promotes the subcellular trafficking of SIRT1 to the nucleus which is necessary for EPO to foster vascular protection. Furthermore, EPO activates Akt1 to phosphorylate FoxO3a and retain this transcription factor in the cytoplasm of ECs to block apoptotic demise. SIRT1 through EPO activation also utilizes mitochondrial pathways to prevent mitochondrial depolarization, cytochrome c release, and Bad, caspase 1, and caspase 3 activation. Our work elucidates a novel relationship between EPO and SIRT1 for the maintenance of vascular integrity during oxidative stress.

MATERIALS AND METHODS

Cerebral Microvascular Endothelial Cell Cultures

All procedures were approved by the Institutional Animal Care and Use Committee of UMDNJ with protocol # 10097. All efforts were made to minimize the number of animals used and their suffering. ECs were isolated from Sprague-Dawley adult rat brain cerebra by using a modified collagenase/dispase-based digestion protocol [2, 5, 53]. Briefly, rat brains were removed and cerebella were cut off aseptically [52, 54]. The cerebral cortices cleaned of white matter were trimmed into blocks (approximately 1-2 mm^3). The blocks were then incubated in dissociation medium containing 1 mg/ml collagenase/dispase (Roche, Mannheim, Germany) in M199E with 0.5% antibiotic-antimycotic solution at 37°C for 2 hours. The cell slurry formed was homogenized and was then re-suspended with 15% dextran (Sigma, Louis, MO, USA). Following centrifugation at 4,000 × g for 20 min (4°C), the pellet was re-suspended in a minimal volume of HEPES buffer and layered onto a pre-prepared colloidal silica gradient solution of 45% Percoll (Sigma, Louis, MO, USA) in Dulbecco's PBS. The upper band (ECs) was collected following centrifugation at 20,000 × g for 20 min (10°C). Cells were re-suspended in growth medium containing 20% heat-inactivated fetal bovine serum, 2 mM L-glutamine, 90 μg/ml heparin, 20 μg/ml endothelial cell growth supplement (ICN Biomedicals, Aurora, OH, USA), and 0.5% antibiotic-antimycotic solution in M199E. The cells were plated on gelatin-coated dishes and continuously incubated in a humidified atmosphere of 5% CO_2 and 95% room air. All experiments were performed using the third passage cells. Endothelial cells were identified by positive direct immunocytochemistry for factor VIII-related antigen [2, 5, 53] and by characteristic spindle-shaped morphology with antigenic properties shown to resemble brain endothelium *in vivo* [55]. All animal experimentation was conducted in accord with accepted standards of humane animal care and NIH guidelines.

Experimental Treatments

Oxygen-glucose deprivation (OGD) in ECs was performed by replacing the media with glucose-free Hank's balanced salt solution containing 116 mmol/l NaCl, 5.4 mmol/l KCl, 0.8 mmol/l $MgSO_4$, 1 mmol/l NaH_2PO_4, 0.9 mmol/l $CaCl_2$, and 10 mg/l phenol red (pH 7.4) and cultures were maintained in an anoxic environment (95% N_2 and 5% CO_2) at 37 °C per the experimental paradigm. For treatments applied prior to OGD, application of EPO (R&D Systems, Minneapolis, MN, USA), resveratrol [3,5,4′ -trihydroxy-*trans*-stilbene) (Tocris Bioscience, Ellisville, MO), or 6-chloro-2,3,4,9-tetrahydro-1*H*-carbazole-1-carboxamide (EX527, Tocris Bioscience, Ellisville, MO) were continuous [56, 57].

Assessment of Cell Survival

EC injury was determined by bright field microscopy using a 0.4% trypan blue dye exclusion method following OGD per our previous protocols [56, 57]. The mean survival was determined by counting eight randomly selected non-overlapping fields with each containing approximately 10-30 cells (viable + non-viable) in each 24 well plate or 35 mm dish.

Assessment of DNA Fragmentation

Genomic DNA fragmentation was determined by the terminal deoxynucleotidyl transferase nick end labeling (TUNEL) assay [12, 58, 59]. Briefly, ECs were fixed in 4% paraformaldehyde/0.2% picric acid/0.05% glutaraldehyde and the 3′-hydroxy ends of cut DNA were labeled with biotinylated dUTP using the enzyme terminal deoxytransferase (Promega, Madison, WI) followed by streptavidin-peroxidase and visualized with 3,3′-diaminobenzidine (Vector Laboratories, Burlingame, CA).

Assessment of Membrane Phosphatidylserine (PS) Residue Externalization

Externalization of membrane PS residues was determined by using Annexin V labeling per our prior studies [45, 47, 58, 59]. A 30 μg/ml stock solution of Annexin V conjugated to phycoerythrin (PE) (R&D Systems, Minneapolis, MN) was diluted to 3 μg/ml in warmed calcium containing binding buffer (10 mmol/L Hepes, pH 7.5, 150 mmol/L NaCl, 5 mmol/L KCl, 1 mmol/L $MgCl_2$, 1.8 mmol/L $CaCl_2$). Plates were incubated with 500 μl of diluted Annexin V for 10 minutes. Images were acquired with "blinded" assessment with a Leitz DMIRB microscope (Leica, McHenry, IL) and a Fuji/Nikon Super CCD (6.1 megapixels) using transmitted light and fluorescent single excitation light at 490 nm and detected emission at 585 nm [12].

Expression of SIRT1, Phosphorylated Akt1, Total Akt1, Phosphorylated FoxO3a, Total FoxO3a, Phosphorylated Bad, and Active Caspase 1 and 3

ECs were homogenized and each sample (50 μg/lane) was subjected to SDS-polyacrylamide gel electrophoresis (7.5% SIRT1, 7.5% Akt1, and FoxO3a; 12.5% Bad, caspase 1 and 3). After transfer, the membranes were incubated with a rabbit polyclonal antibody against SIRT1 (1:200, Santa Cruz Biotechnologies, Santa Cruz, CA), a rabbit polyclonal antibody against phospho-Akt1 (Ser^{473}, 1:1000, Cell Signaling, Beverly, MA), a rabbit antibody against total Akt1, a rabbit polyclonal antibody against phospho-FoxO3a (1:1000) (p-FoxO3a, Ser^{253}, Cell Signaling, Beverly, MA), a rabbit antibody against total FoxO3a, a rabbit monoclonal antibody against phospho-Bad (Ser^{136}, 1:1000, Cell Signaling, Beverly, MA), and a rabbit antibody against cleaved (active) caspase 1 (20 kDa) (1:1000), or a rabbit antibody against cleaved (active) caspase 3 (17 kDa) (1:1000) (Cell signaling Technology, Beverly, MA). Following washing, the membranes were incubated with a horseradish peroxidase (HRP) conjugated secondary antibody goat anti-rabbit IgG (1:2000, Zymed Laboratories, Carlsbad, CA). The antibody-reactive bands were revealed by

chemiluminescence (Amersham Pharmacia Biotech, Piscataway, NJ) and band density was performed using the public domain NIH Image program (developed at the U.S. National Institutes of Health and available at http://rsb.info.nih.gov/nih-image/).

SIRT1 Histone Deacetylase (HDAC) Activity Assay

Per our prior protocols [52], ECs were homogenized and following protein determination, each sample (30 μg/10 μl) was used for SIRT1 activity measurement. SIRT1 histone deacetylase (HDAC) activity was determined with the use of SIRT1 Fluorimetric Drug Discovery Kit (Biomol International, Plymouth Meeting, PA) and following the manufacturer's protocol. EC protein extracts were incubated in assay buffer with ß-nicotinamide adenine dinucleotide (NAD^+) substrate at 37°C for 45 minutes. The fluorescence density was determined using a Multimode Detector (DTX880, Beckman Coulter, Brea, CA) and the relative activity of SIRT1 compared to untreated control ECs was used in the results.

Gene Silencing of *SIRT1* with Small Interfering RNA (siRNA)

To silence *SIRT1* gene expression, the following sequences were synthesized (Applied Biosystems, Foster City, CA): the SIRT1 siRNA sense strand 5′-GCGAUGUUAUAAUUAAUGAtt-3′ and the antisense strand 5′-UCAUUAAUUAUAACAUCGCag-3′. Transfection of siRNA duplexes was performed with Lipofectamine 2000 reagent according to manufacturer guidelines (Invitrogen, Carlsbad, CA). Experimental assays were performed 72 hours post-transfection. For each siRNA assay, positive controls contain multiple siRNAs including the target siRNA and negative controls are absent of the target siRNA. In addition, following gene knockdown of *SIRT1*, the expression of these proteins was assessed by immunofluorescence and western analysis. EC cultures were incubated with rabbit anti-SIRT1 (1:100, Santa Cruz Biotechnologies, Santa Cruz, CA) at 4°C over night. After incubation with biotinylated anti-rabbit IgG (1:50) (Vector Laboratories, Burlingame, CA) at room temperature for 2 hours, the expression was revealed by conjugation to fluorescein avidin (1:50) (Vector Laboratories, Burlingame, CA) [52].

Assessment of Mitochondrial Membrane Potential

The fluorescent probe JC-1 (Molecular Probes, Eugene, OR), a cationic membrane potential indicator, was used to assess the mitochondrial membrane potential [46, 60]. ECs in 35 mm dishes were incubated with 2 μg/ml JC-1 in growth medium at 37 °C for 30 min. The cultures were washed three times using fresh growth medium. Mitochondria were then analyzed immediately under a Leitz DMIRB microscope (Leica, McHenry, IL, USA) with a dual emission fluorescence filter with 515-545 nm for green fluorescence and emission at 585-615 nm for red fluorescence [58].

Preparation of Mitochondria for the Analysis of Cytochrome c Release

After washing once with ice-cold PBS, cells were harvested at 10,000g for 15 min at 4°C and the resulting pellet was re-suspended in buffer A (20 mM HEPES, pH 7.5, 10 mM KCl, 1.5 mM $MgCl_2$, 1 mM EDTA, 1 mM EGTA, 1 mM dithiothreitol, 0.1 phenylmethylsulfonylfluoride) containing 250 mM sucrose and used as the mitochondrial fraction. The supernatant was subjected to ultracentrifugation at 50,000 g for 1 hour at 4 °C with the resultant supernatant used as the cytosolic fraction [61].

Immunocytochemistry for SIRT1, FoxO3a, and Caspase 3

Per our prior protocols [52, 54, 56, 57, 62], for immunocytochemical staining of SIRT1, FoxO3a, or cleaved caspase 3 (active form), ECs were fixed with 4% paraformaldehyde and

permeabilized using 0.2% Triton X-100. Cells were then incubated with rabbit anti-SIRT1 (1:100, Santa Cruz Biotechnologies, Santa Cruz, CA), anti-FoxO3a (1:100, Cell Signaling Technology, Beverly, MA) or rabbit anti-cleaved caspase 3 (1:200, Cell Signaling Technology, Beverly, MA) over night at 4 °C and then with biotinylated anti-rabbit IgG (1:50, Vector laboratories) for 2 hours followed by Texas Red streptavidin (1:50, Vector laboratories) for 1 hour. Cells were washed in PBS, then stained with DAPI (Sigma, St. Louis, MO) for nuclear identification. SIRT1, FoxO3a, and caspase 3 proteins were imaged with fluorescence at the wavelengths of 565 nm (red) and 400 nm (DAPI nuclear staining).

Subcellular Translocation of SIRT1 or FoxO3a by Western Analysis

Per our prior protocols [5, 52], ECs were initially homogenized. The cytoplasmic and nuclear proteins were subsequently prepared by using NE-PER nuclear and cytoplasmic extraction reagents according to the instructions of the manufacturer (Pierce, Rockford, IL). The expression of SIRT1 or FoxO3a in the EC nucleus and cytoplasm was determined by Western analysis. Each sample (50 μg/lane) was subjected to 7.5% SDS-polyacrylamide gel electrophoresis. After transfer, the membranes were incubated with a rabbit polyclonal antibody against SIRT1 (1:200) (Santa Cruz Biotechnologies, Santa Cruz, CA) or a primary rabbit antibody against FoxO3a (1:1000) (Cell Signaling, Beverly, MA). After washing, the membranes were incubated with a horseradish peroxidase conjugated with a secondary antibody (goat anti-rabbit IgG, 1:2000) (Invitrogen, Carlsbad, CA). The antibody-reactive bands were revealed by chemiluminescence (Amersham Pharmacia Biotech, Piscataway, NJ) and band density was performed using the public domain NIH Image program (developed at the U.S. National Institutes of Health and available at http://rsb.info.nih.gov/nih-image/).

Statistical Analysis

For each experiment, the mean and standard error were determined. Statistical differences between groups were assessed by means of analysis of variance (ANOVA) from 6 replicate experiments with the post-hoc Dunnett's test. Statistical significance was considered at $P<0.05$.

RESULTS

Oxygen-Glucose Deprivation (OGD) Results in Progressive EC Injury

We investigated EC survival after exposure to OGD at various periods of exposure of 6 hours, 8 hours, and 12 hours. Cell survival was assessed with trypan blue exclusion 24 hours after OGD exposure. As shown in Fig. (**1A**), representative pictures demonstrate that exposure to OGD for 6, 8 or 12 hours results in a loss of membrane integrity and staining in a significant number of ECs cells with trypan blue dye exclusion method. The quantitative results demonstrate that EC survival was significantly decreased to 57 ± 6% (6 hours), 39 ± 4% (8 hours), and 12 ± 4% (12 hours) after OGD when compared to untreated control cultures (97 ± 8%) (Fig. **1B**). Since OGD exposure for a period of 8 hours resulted in survival rate of approximately 39% (61% EC loss), this duration of OGD was used for the reminder of the experimental paradigms.

EPO Protects Against OGD Cell Death and Apoptotic Demise

We next examined the ability of EPO to alter EC injury following OGD exposure. EPO at a series of concentrations (0.1~100 ng/ml) was applied to EC cultures 1 hour prior to the administration of OGD and cell survival was determined 24 hours later by using trypan blue exclusion method. As shown in Fig. (**1C**), EPO at the concentrations of 1, 10, and 50 ng/ml significantly reduced trypan blue uptake in ECs and the concentration of 10 ng/ml provided

the maximal EC survival, which was used for the subsequent experiments. Concentrations lower than 0.1 ng/ml or higher than 50 ng/ml did not improve EC survival during OGD (Fig. **1C**).

At 24 hours after OGD exposure, apoptotic DNA fragmentation and phosphatidylserine (PS) exposure were assessed by TUNEL assay and Annexin V labeling method respectively. As shown in Fig. 1D, the quantitative results indicated that percent cell injury, DNA fragmentation, and percent PS exposure were significantly increased following OGD exposure, but EPO (10 ng/ml) pretreatment significantly reduced percent cell injury, DNA fragmentation and PS exposure to 28 ± 3%, 28 ± 2%, and 20 ± 5% respectively.

EPO Enhances Endogenous SIRT1 Activity and Fosters SIRT1 Shuttling to the Nucleus

We next examined an activator of SIRT1 with resveratrol (15 μM) and the specific small-molecule inhibitor of SIRT1 catalytic activity EX527 (2 μM) [63] to alter SIRT1 activity assessed by HDAC activity at 6 hours and 24 hours following OGD exposure (Fig. **1E**). Gene knockdown of *SIRT1* also was performed with siRNA. Over a 24 hour course, OGD exposure led to a decrease in SIRT1 activity to 0.57 ± 0.10. However, resveratrol (15 μM) significantly increased HDAC activity similar to EPO (10 ng/ml) increasing SIRT1 activity. The SIRT1 inhibitor EX527 (2 μM) decreased HDAC activity significantly at 24 hours to 0.38 ± 0.10. In addition, gene knockdown of *SIRT1* by SIRT1 siRNA also decreased HDAC activity at 6 and 24 hours to 0.15 ± 0.10 and 0.13 ± 0.10 respectively. More importantly, the effect of EPO on HDAC activity was abolished by either EX527 or SIRT1 siRNA transfection at 6 hours and 24 hours (Fig. **1E**).

We next examined the cellular trafficking of SIRT1 in ECs after OGD (Figs. **2A, 2B**). In some scenarios, loss of SIRT1 endogenous cellular expression may result in cell injury during toxin exposure [45, 47] and nuclear translocation of SIRT1 may be necessary for cell survival and growth [48, 64]. We employed immunofluorescent staining for SIRT1 and DAPI nuclear staining to follow the translocation of SIRT1 at 6 hours after OGD. Untreated control ECs in merged images do not have visible nuclei (red in color, white arrows), suggesting that SIRT1 is present in both cytoplasmic and nuclear locations. After OGD exposure, a significant proportion of SIRT1 is confined to the cytoplasm of ECs as illustrated by minimal nuclear red staining with contrasting marked DAPI staining (blue nuclei in color) in the nucleus in ECs in merged images. In contrast, administration of EPO (10 ng/ml) or resveratrol (RES, 15 μM) fostered the translocation of endogenous SIRT1 from the cytoplasm to the nucleus, which is illustrated by the inability to detect significant DAPI nuclear staining (blue in color) in cells during merged elevated images since SIRT1 staining overlapped DAPI staining in ECs. Application of the specific SIRT1 inhibitor EX527 (2 μM) during OGD prevented the nuclear translocation of SIRT1 and retained SIRT1 in the cytoplasm of ECs to a greater degree than during periods with OGD alone. Application of EPO alone or in combination with resveratrol led to similar levels of nuclear localization of SIRT1, but inhibition of SIRT1 catalytic activity with EX527 prevented EPO from fostering nuclear localization of SIRT1.

We also examined SIRT1 subcellular translocation from the cell cytoplasm to the nucleus through western analysis (Figs. **2C, 2D**). At 24 hours following OGD, SIRT1 remained confined to the cytoplasm of ECs, but resveratrol, EPO, or combined resveratrol and EPO resulted in significant nuclear localization of SIRT1. Yet, inhibition of SIRT1 catalytic activity with EX527 (2 μM) markedly reduced the translocation of SIRT1 to the nucleus and maintained SIRT1 in the cytoplasm of ECs to a greater extent than during OGD alone and during EPO administration.

Activation of SIRT1 is Necessary and Sufficient for EPO to Protect ECs during OGD

Western blot assay was performed for the endogenous cellular expression of SIRT1 following OGD. In Fig. (**3A**), expression of endogenous SIRT1 was progressively decreased over 24 hours after OGD exposure. EPO (10 ng/ml) application prior to OGD prevented the decrease in the SIRT1 expression at 1, 6 and 24 hours following OGD. Yet, transfection with SIRT1 siRNA in ECs resulted in significant reduction of the expression of SIRT1 protein as revealed with Western blot analysis and immunocytochemistry at 6 hours after OGD (Figs. **3B** and **3C**). As a control, non-specific scrambled siRNA did not alter SIRT1 protein expression in untreated control cells or cells exposed to OGD, illustrating the specificity of SIRT1 siRNA to block protein expression of SIRT1.

To investigate whether SIRT1 activation is required for EPO protection, EC cell survival and apoptosis were assessed with trypan blue staining, apoptotic genomic DNA fragmentation (TUNEL), and membrane PS exposure (annexin V staining) 24 hours following OGD. As shown in Fig. (**4**), representative images (Figs. **4A** and **4C**) demonstrate that untreated control ECs were with minimal trypan blue, TUNEL or annexin V staining. In contrast, OGD led to a significant increase in trypan blue staining, DNA fragmentation and membrane PS exposure in ECs 24 hours after OGD. Inhibition of SIRT1 activity with EX527 (2 μM) or during gene knockdown of *SIRT1* with siRNA significantly increased cell injury, DNA fragmentation, and PS membrane exposure following OGD when compared with OGD alone. Transfection with non-specific scrambled siRNA did not alter cell injury. Application of EPO (10 ng/ml), resveratrol (RES 15 μM) or combined EPO and resveratrol given 1 hr prior to OGD significantly reduced trypan blue staining, DNA fragmentation, and membrane PS exposure to a similar degree, suggesting that EPO and resveratrol were relying upon a similar protective pathway that involved SIRT1. In further support of this, protection by EPO was significantly reduced during inhibition of SIRT1 with EX527 or during *SIRT1* gene knockdown. Quantification of results (Figs. **4B** and **4D**) illustrate that OGD led to a significant increase in percent trypan blue staining (56 ± 2%), DNA fragmentation (55 ± 3%) and membrane PS exposure (54 ± 6%) in ECs 24 hours after OGD when compared to untreated control cultures for trypan blue staining (3 ± 2%), for DNA (4 ± 2%) and for PS (3 ± 2%) respectively. EC injury was further increased by EX527 (2 μM) or gene knockdown of *SIRT1* with siRNA. Application of EPO (10 ng/ml), resveratrol (RES 15 μM), or combined EPO and resveratrol therapy significantly decreased percent trypan blue staining, DNA fragmentation, and membrane PS exposure. As noted above, protection with EPO was markedly reduced during SIRT1 inhibition with SIRT1 inhibitor EX527 or with SIRT1 siRNA transfection.

EPO Relies upon SIRT1 to Activate Akt1, Phosphorylate FoxO3a, and Retain FoxO3a in the Cytoplasm of ECs during OGD

Western blot assay was performed for EC expression of phosphorylated FoxO3a, total FoxO3a, phosphorylated Akt1 and total Akt1 following OGD exposure. Expression of phosphorylated (inactive) p-FoxO3a was significantly increased at 6 hours and subsequently decreased at 24 hours after OGD exposure (Fig. **5A**). EPO (10 ng/ml) maintained the expression of phosphorylated FoxO3a at 1,6 and 24 hours to a greater degree than OGD exposure alone.

We next examined the activation and phosphorylation of Akt1 by EPO, resveratrol, and during SIRT1 inhibition. Akt1 modulates the phosphorylation of FoxO3a that can inhibit its activity [43, 65]. Without Akt, FoxO3a can remain unphosphorylated and active to translocate to the cell nucleus to result in apoptosis [5, 66]. Since unphosphorylated FoxO3a can translocate to the cell nucleus and not be bound by 14-3-3 proteins [17, 54], we examined the ability of EPO and SIRT1 pathways to modulate post-translational

phosphorylation of Akt1. As shown in Figs. (**5B** and **5C**), Akt1 phosphorylation at 6 hours during OGD was significantly increased by EPO (10 ng/ml), resveratrol (15 μM), or combined EPO and resveratrol administration to a greater degree than by exposure to OGD alone. Inhibition of SIRT1 activity with EX527 (2 μM) or gene knockdown of *SIRT1* with siRNA resulted in significantly decreased expression of phosphorylated Akt1 during OGD exposure as well as during EPO administration, suggesting that EPO increases Akt1 activity through SIRT1.

Since EPO was able to maintain inhibitory phosphorylation of FoxO3a through increased Akt1 activity that was dependent upon SIRT1, we next examined whether EPO controlled subcellular trafficking of FoxO3a through a SIRT1 dependent mechanism. We performed immunofluorescent staining for FoxO3a with DAPI nuclear staining to follow the subcellular translocation of FoxO3a at 6 hours after OGD exposure (Figs. **6A** and **6C**). In the presence of OGD, immunofluorescent staining for FoxO3a in the nucleus of ECs is markedly present. This is demonstrated by the inability to visualize DAPI nuclear staining (blue in color) in ECs during merged images since significant FoxO3a staining is present in the nucleus (Figs. **6A** and **6C**). In addition, either inhibition of SIRT1 activity with EX527 (2 μM) or gene knockdown of *SIRT1* during OGD also allowed the translocation of FoxO3a from the cell cytoplasm to the nucleus in ECs (Fig. **6A**) and yielded significantly greater nuclear translocation of FoxO3a than OGD alone (Fig. **6A**). Furthermore, EPO (10 ng/ml), resveratrol (RES 15 μM) or combined EPO and resveratrol therapy maintained FoxO3a in the cytoplasm of ECs similar to untreated control cells, demonstrating minimal nuclear staining as shown with DAPI staining (blue nuclei in color) in the nucleus of merged images (Figs. **6A** and **6C**). To complement the immunofluorescent studies with assessment of FoxO3a subcellular translocation from the cell cytoplasm to the nucleus, western analysis results were consistent with our immunofluorescent work demonstrating that application EPO (10 ng/ml), resveratrol (RES 15 μM), or combined EPO with resveratrol therapy prevented translocation of FoxO3a in the nucleus during OGD and maintained FoxO3a in the cytoplasm of ECs. In contrast, co-application of EX527 (2 μM) or transfection with SIRT1 siRNA increased the subcellular trafficking of FoxO3a to the nucleus of ECs (Figs. **6B** and **6D**).

EPO Utilizes SIRT1 to Prevent Mitochondrial Depolarization, Cytochrome c Release, and Activation of Bad in ECs during OGD

Mitochondrial depolarization in ECs was assessed during OGD by the cationic membrane potential indicator JC-1. In Figs. (**7A** and **7B**), OGD yielded a significant decrease in EC mitochondrial red/green fluorescence intensity ratio at 6 hours after OGD (44 ± 5%) when compared to untreated control mitochondria (100 ± 6%), suggesting that OGD results in mitochondrial membrane depolarization. Inhibition of SIRT1 activity with EX527 (2 μM) or gene knockdown of *SIRT1* with siRNA (Figs. **7A** and **7B**) during OGD further decreased mitochondrial membrane red/green fluorescence ratio to 20 ± 2% and 20 ± 3% respectively. Non-specific scrambled siRNA did not change mitochondrial depolarization during OGD when compared to OGD alone (Fig. **7A**). Yet, EPO (10 ng/ml), resveratrol (RES 15 μM), or combined EPO and resveratrol therapy given 1 hour prior to OGD significantly increased the red/green fluorescence intensity of the mitochondria to 77 ± 4%, 76 ± 3%, and 80 ± 3% respectively to block mitochondrial depolarization. Yet, the ability of EPO to modulate mitochondrial depolarization was dependent upon the presence of SIRT1 activity since application of EX527 (2 μM) or gene knockdown of *SIRT1* with siRNA negated the ability of EPO to maintain mitochondrial polarization (Figs. **7A** and **7B**).

Subsequent cytochrome c release from mitochondria was evaluated by Western blot for cytochrome c expression in both mitochondrial and cytosol extractions. As shown in Figs. (**7C** and **7D**), OGD increased expression of cytochrome c in the cytosolic fractions. More

intense release of cytochrome c into the cytosol was present during OGD and inhibition of SIRT1 with EX527 (2 μM) or transfection with SIRT1 siRNA (Fig. **7C**). Non-specific scrambled siRNA did not alter cytochrome c expression during OGD exposure (Fig. **7C**). In contrast, EPO (10 ng/ml), resveratrol (RES 15 μM), or combined EPO and resveratrol therapy prevented cytochrome c release from the mitochondria to equal degrees, suggesting reliance upon SIRT1 pathways. Treatment with EX527 (2 μM) or SIRT1 siRNA eliminated the ability of EPO to maintain cytochrome c in the mitochondrial fraction (Figs. **7C** and **7D**).

Since EPO is dependent upon SIRT1 to control mitochondrial depolarization and the release of cytochrome c, we hypothesized that EPO through SIRT1 pathways also may modulate phosphorylation of Bad. Bad is localized in the outer mitochondrial membrane and when phosphorylated by Akt1 can bind to protein 14-3-3 to release Bcl-x_L and prevent apoptosis [39, 46, 49, 67, 68]. Western blot assay was performed for phosphorylated Bad (p-Bad) at the preferential phosphorylation site (Ser^{136}) of Akt1 (Figs. **7E** and **7F**). The expression of phospho-Bad (p-Bad) was significantly reduced at 6 hours after OGD exposure. Application of EPO (10 ng/ml), resveratrol (RES 15 μM), or combined EPO and resveratrol therapy prior to OGD significantly increased the expression of p-Bad. Yet, SIRT1 inhibition with EX527 (2 μM) or gene knockdown with SIRT1 siRNA decreased p-Bad expression and antagonized the ability of EPO to phosphorylate Bad (Figs. **7E** and **7F**).

EPO through SIRT1 Blocks Caspase 1 and Caspase 3 Activation During OGD Exposure

With our present data, we show that EPO relies upon SIRT1 to modulate mitochondrial membrane permeability and cytochrome c release. Therefore, we next examined whether EPO requires SIRT1 to control caspase 1 and caspase 3 activities since mitochondrial release of cytochrome c is a major pathway leading to apoptotic caspase activation [67, 69-72]. Immunocytochemistry analysis for caspase 3 demonstrates significant cleaved (active) caspase 3 (red) staining) at 6 hours after OGD exposure, during the inhibition of SIRT1 activity with EX527 (2 μM), or during gene knockdown of *SIRT1* with siRNA. Non-specific scrambled siRNA did not alter caspase 3 activity during OGD. Application of EPO (10 ng/ml), resveratrol (RES 15 μM), or combined therapy with EPO and resveratrol during OGD significantly blocked caspase 3 activity as evidenced by primarily blue immunocytochemical staining and by reducing the percentage of cleaved caspase 3 labeling to 21 ± 2%, 23 ± 3% and 20 ± 4% respectively from 52 ± 4% in ECs exposed to OGD alone (Figs. **8A** and **8B**). Our data also suggests that EPO requires SIRT1 activity to limit caspase 3 activity, since the ability of EPO to modulate caspase 3 activity was lost during application of the SIRT1 inhibitor EX527 (2 μM) or *SIRT1* siRNA gene knockdown with EPO exposure.

In Figs. (**8C** and **8D**), the expression of cleaved (active) caspase 3 and caspase 1 on western analysis were significantly increased at 6 hours after OGD exposure. Transfection with SIRT1 siRNA or inhibition of SIRT1 activity with EX527 (2 μM) resulted in a significant elevation in caspase 3 and caspase 1 activities, suggesting that endogenous SIRT1 in ECs offers underlying protection against the apoptotic activation of caspase 3 and caspase 1 (Figs. **8C** and **8D**). Non-specific scrambled siRNA did not alter caspase 3 and caspase 1 activities during OGD exposure, further supporting the specific ability of SIRT1 to control caspase 3 and caspase 1 activities. EPO (10 ng/ml), resveratrol (RES 15 μM), or combined EPO and resveratrol therapy significantly blocked caspase 3 and caspase 1 activity during OGD. However, the ability of EPO to limit caspase 3 and caspase 1 activity during OGD was lost during combined application of the SIRT1 inhibitor EX527 (2 μM) or during transfection with SIRT1 siRNA (Figs. **8C** and **8D**).

DISCUSSION

In the present study, we demonstrate that EPO can reduce oxidative injury in cerebral microvascular ECs in a dose dependent manner. We show that OGD exposure for a period of 8 hours leads to a significant decrease in EC survival and an increase in apoptotic membrane PS externalization and nuclear DNA fragmentation when compared to control ECs. The concentration of EPO to provide cytoprotection was most effective at 10 ng/ml and was consistent with prior studies [4, 5, 23, 24, 73]. As previously described [12], this concentration is similar to serum levels of EPO during cardiac or renal disease that may assist with cellular survival [74, 75] since clinical applications of EPO increase plasma EPO levels significantly above the 1.0 ng/ml range offer beneficial outcomes [76, 77]. In addition, EPO blocks apoptotic DNA degradation and PS exposure in ECs during oxidative stress to a similar degree as seen in cardiac and vascular cell models [2, 5, 78, 79]. DNA fragmentation and PS exposure can represent a continuum of apoptotic injury [13, 67, 80] with inflammatory cell activation that eliminates ECs tagged with PS [58, 81-83].

SIRT1 can play an important role during EC function and survival. For example, activation of SIRT1 also can prevent endothelial senescence [50] and reduce endothelial atherosclerotic lesions during elevated lipid states [84], and prevent oxidative stress injury [52, 85]. We show that endogenous SIRT1 expression in ECs is lost over 24 hours following OGD exposure, but EPO can maintain the expression of SIRT1 during oxidative stress. Loss of SIRT1 activity, such as during inhibition with SIRT1 inhibitor (EX527) or during gene knockdown of *SIRT1*, results in significant EC injury and loss of EPO cytoprotection, suggesting that endogenous SIRT1 in ECs is important for EC survival. In addition, SIRT1 activity is necessary and sufficient for EPO to protect ECs against OGD. SIRT1 is primarily a nuclear protein [49, 86], but can shuttle between the cell nucleus and cytoplasm and may be necessary for cell survival and differentiation [48, 64]. With evidence through both western analysis and immunocytochemistry, we demonstrate that EPO or resveratrol maintains SIRT1 in the nucleus of ECs. However, in the absence of EPO during non-cytoprotective oxidative stress protocols alone or during blockade of SIRT1 catalytic activity SIRT1 with EX527 remains confined to the cytoplasm of ECs.

EPO relies upon SIRT1 for the activation of Akt1, the phosphorylation of FoxO3a, and the maintenance of FoxO3a in the cytoplasm of ECs. Activation of SIRT1 results in cellular protection [52, 85] and has been associated with enhanced activity of Akt [46, 51, 87]. Akt1 can phosphorylate FoxO3a and block its activity [25, 43, 65, 88], but in the absence of Akt1 activity FoxO3a translocates to the cell nucleus for apoptotic injury [5, 66]. We demonstrate that EPO or resveratrol leads to SIRT1 activation of Akt1, phosphorylation of FoxO3a, and retention of FoxO3a in the cytoplasm of ECs during oxidative stress. Loss of SIRT1 activity through pharmacological inhibition or gene knockdown results in the loss of EPO to control Akt1 activity and phosphorylation of FoxO3a. EPO by activating SIRT1 phosphorylates FoxO3a prevents the subcellular trafficking of FoxO3a from the cytoplasm to the EC nucleus. In other studies, unphosphorylated (active) FoxO3a is able to disassociate from 14-3-3 proteins in the cytosol of cells and translocate to the cell nucleus to initiate apoptotic transcriptional activity [5, 66].

EPO through SIRT1 also may rely upon the maintenance of mitochondrial membrane permeability, which is a significant mechanism to preserve cell survival [52, 89, 90]. Agents, such as resveratrol that activate sirtuins can reduce mitochondrial reactive oxygen species [85, 91, 92]. Our work demonstrates that EPO, resveratrol, and SIRT1 activation prevents mitochondrial membrane depolarization following OGD exposure and the release of cytochrome c in ECs. In contrast, inhibition of SIRT1 activity or gene knockdown of

SIRT1 results in significant mitochondrial membrane permeability and the release of cytochrome c.

Since EPO is dependent upon SIRT1 to control mitochondrial depolarization and the release of cytochrome c, we next investigated whether EPO through SIRT1 pathways also may modulate the phosphorylation of Bad. SIRT1 independently can activate and increase the phosphorylation of Bad during experimental diabetes [52]. Bad is localized on the outer mitochondrial membrane and binds to the anti-apoptotic Bcl-2 family member Bcl-x_L through its BH3 domain and release Bcl-x_L following phosphorylation by Akt1 to prevent mitochondrial dysfunction [39, 46, 49, 67, 68]. Our work shows that EPO and resveratrol requires SIRT1 to significantly increase the phosphorylation of Bad during OGD. Loss of SIRT1 during gene knockdown or inhibition of SIRT1 activity decreases the ability of EPO to phosphorylate Bad, demonstrating that SIRT1 is a significant component for EPO to maintain the activity of Bad during oxidative stress.

SIRT1 can reduce caspase activity following loss of mitochondrial permeability in other cell systems such as chondrocytes [93] and retinal cells [94]. Furthermore, EPO alone can modulate caspase activity [2, 3, 12, 38, 69, 95, 96]. As a result, we examined the ability of EPO through SIRT1 to control apoptotic caspase 3 and caspase 1 activities in ECs during OGD. We demonstrate that elevated OGD activates caspase 3 and caspase 1, but that EPO, resveratrol, and SIRT1 activation significantly attenuates caspase 3 and 1 activities. Yet, blockade of SIRT1 activity or gene knockdown of *SIRT1* enhances the activities of these proteases, illustrating that EPO through SIRT1 prevents caspase activation.

It is vital to elucidate the cellular mechanisms of protection for EPO in cerebral ECs. Our present study demonstrates that EPO regulates SIRT1 activity to govern apoptotic injury programs including early PS membrane and late DNA fragmentation. These pathways are mediated through Akt1, phosphorylation and nuclear trafficking of FoxO3a, mitochondrial membrane permeability, cytochrome c release, Bad activity, and caspase 1 and caspase 3 activities. Our work highlights a novel association between EPO and SIRT1 in the regulation of apoptotic pathways in ECs.

Acknowledgments

This research was supported by the following grants to Kenneth Maiese: American Diabetes Association, American Heart Association (National), Bugher Foundation Award, Janssen Neuroscience Award, LEARN Foundation Award, MI Life Sciences Challenge Award, Nelson Foundation Award, NIH NIEHS (P30 ES06639), NIH NIA, NIH NINDS, and NIH ARRA.

REFERENCES

[1]. Bonofiglio R, Lofaro D, Greco R, Senatore M, Papalia T. Proteinuria is a predictor of posttransplant anemia. Transplant Proc. May; 2011 43(4):1063–6. [PubMed: 21620053]

[2]. Chong ZZ, Kang JQ, Maiese K. Erythropoietin is a novel vascular protectant through activation of Akt1 and mitochondrial modulation of cysteine proteases. Circulation. Dec 3; 2002 106(23): 2973–9. [PubMed: 12460881]

[3]. Chong ZZ, Kang JQ, Maiese K. Apaf-1, Bcl-xL, Cytochrome c, and Caspase-9 Form the Critical Elements for Cerebral Vascular Protection by Erythropoietin. J Cereb Blood Flow Metab. Mar; 2003 23(3):320–30. [PubMed: 12621307]

[4]. Chong ZZ, Kang JQ, Maiese K. Erythropoietin fosters both intrinsic and extrinsic neuronal protection through modulation of microglia, Akt1, Bad, and caspase-mediated pathways. Br J Pharmacol. Mar; 2003 138(6):1107–18. [PubMed: 12684267]

[5]. Chong ZZ, Maiese K. Erythropoietin involves the phosphatidylinositol 3-kinase pathway, 14-3-3 protein and FOXO3a nuclear trafficking to preserve endothelial cell integrity. Br J Pharmacol. Apr; 2007 150(7):839–50. [PubMed: 17339844]

[6]. Chong ZZ, Shang YC, Maiese K. Vascular injury during elevated glucose can be mitigated by erythropoietin and Wnt signaling. Curr Neurovasc Res. Aug; 2007 4(3):194–204. [PubMed: 17691973]

[7]. Colella P, Iodice C, Di Vicino U, Annunziata I, Surace EM, Auricchio A. Non-erythropoietic erythropoietin derivatives protect from light-induced and genetic photoreceptor degeneration. Hum Mol Genet. Jun 1; 2011 20(11):2251–62. [PubMed: 21421996]

[8]. Loeliger MM, Mackintosh A, De Matteo R, Harding R, Rees SM. Erythropoietin protects the developing retina in an ovine model of endotoxin-induced retinal injury. Invest Ophthalmol Vis Sci. May; 2011 52(5):2656–61. [PubMed: 21245409]

[9]. Mastromarino V, Volpe M, Musumeci MB, Autore C, Conti E. Erythropoietin and the heart: facts and perspectives. Clin Sci (Lond). Jan; 2011 120(2):51–63. [PubMed: 20929439]

[10]. Moore EM, Bellomo R, Nichol AD. Erythropoietin as a novel brain and kidney protective agent. Anaesth Intensive Care. May; 2011 39(3):356–72. [PubMed: 21675055]

[11]. Rorth M, Madsen KR, Burmolle SH, et al. Effects of Darbepoetin Alfa with exercise in cancer patients undergoing chemotherapy: an explorative study. Scand J Med Sci Sports. Jun; 2011 21(3):369–77. [PubMed: 20136754]

[12]. Chong ZZ, Hou J, Shang YC, Wang S, Maiese K. EPO Relies upon Novel Signaling of Wnt1 that Requires Akt1, FoxO3a, GSK-3beta, and beta-Catenin to Foster Vascular Integrity During Experimental Diabetes. Curr Neurovasc Res. May 1; 2011 8(2):103–20. [PubMed: 21443457]

[13]. Maiese K. Diabetic stress: new triumphs and challenges to maintain vascular longevity. Expert Rev Cardiovasc Ther. Mar; 2008 6(3):281–4. [PubMed: 18327989]

[14]. Maiese, K.; Chong, Z.; Li, F. Reducing oxidative stress and enhancing neurovascular longevity during diabetes mellitus. In: Maiese, K., editor. Neurovascular Medicine: Pursuing Cellular Longevity for Healthy Aging. Oxford University Press; New York, NY: 2009. ISBN13: 978-0-19-532669-7, ISBN10: 0-19-532669-5:540-64

[15]. Maiese K, Chong ZZ, Hou J, Shang YC. Erythropoietin and oxidative stress. Curr Neurovasc Res. May; 2008 5(2):125–42. [PubMed: 18473829]

[16]. Maiese K, Chong ZZ, Shang YC. Mechanistic insights into diabetes mellitus and oxidative stress. Curr Med Chem. 2007; 14(16):1729–38. [PubMed: 17627510]

[17]. Maiese K, Shang YC, Chong ZZ, Hou J. Diabetes mellitus: channeling care through cellular discovery. Curr Neurovasc Res. Feb 1; 2010 7(1):59–64. [PubMed: 20158461]

[18]. Warren JS, Zhao Y, Yung R, Desai A. Recombinant human erythropoietin suppresses endothelial cell apoptosis and reduces the ratio of bax to bcl-2 proteins in the aortas of apolipoprotein e-deficient mice. J Cardiovasc Pharmacol. Apr; 2011 57(4):424–33. [PubMed: 21242808]

[19]. Lombardero M, Kovacs K, Scheithauer BW. Erythropoietin: a hormone with multiple functions. Pathobiology. 2011; 78(1):41–53. [PubMed: 21474975]

[20]. Maiese K, Chong ZZ, Li F, Shang YC. Erythropoietin: elucidating new cellular targets that broaden therapeutic strategies. Prog Neurobiol. Jun; 2008 85(2):194–213. [PubMed: 18396368]

[21]. Maiese K, Li F, Chong ZZ. Erythropoietin in the brain: can the promise to protect be fulfilled? Trends Pharmacol Sci. 2004; 25(11):577–83. 11. [PubMed: 15491780]

[22]. Maiese K, Li F, Chong ZZ. New avenues of exploration for erythropoietin. Jama. Jan 5; 2005 293(1):90–5. [PubMed: 15632341]

[23]. Chong ZZ, Li F, Maiese K. Erythropoietin requires NF-kappaB and its nuclear translocation to prevent early and late apoptotic neuronal injury during beta-amyloid toxicity. Curr Neurovasc Res. Dec; 2005 2(5):387–99. [PubMed: 16375720]

[24]. Chong ZZ, Lin SH, Kang JQ, Maiese K. Erythropoietin prevents early and late neuronal demise through modulation of Akt1 and induction of caspase 1, 3, and 8. J Neurosci Res. Mar 1; 2003 71(5):659–69. [PubMed: 12584724]

[25]. Chong ZZ, Shang YC, Zhang L, Wang S, Maiese K. Mammalian target of rapamycin: hitting the bull's-eye for neurological disorders. Oxid Med Cell Longev. Nov-Dec; 2010 3(6):374–91. [PubMed: 21307646]

[26]. Kollensperger M, Krismer F, Pallua A, Stefanova N, Poewe W, Wenning GK. Erythropoietin is neuroprotective in a transgenic mouse model of multiple system atrophy. Mov Disord. Feb 15; 2011 26(3):507–15. [PubMed: 21462262]

[27]. Keogh CL, Yu SP, Wei L. The effect of recombinant human erythropoietin on neurovasculature repair after focal ischemic stroke in neonatal rats. J Pharmacol Exp Ther. Aug; 2007 322(2):521–8. [PubMed: 17494864]

[28]. Li Y, Lu Z, Keogh CL, Yu SP, Wei L. Erythropoietin-induced neurovascular protection, angiogenesis, and cerebral blood flow restoration after focal ischemia in mice. J Cereb Blood Flow Metab. May; 2007 27(5):1043–54. [PubMed: 17077815]

[29]. Maiese K, Chong ZZ, Hou J, Shang YC. Oxidative stress: Biomarkers and novel therapeutic pathways. Exp Gerontol. Mar; 2010 45(3):217–34. [PubMed: 20064603]

[30]. Schmeding M, Neumann UP, Boas-Knoop S, Spinelli A, Neuhaus P. Erythropoietin reduces ischemia-reperfusion injury in the rat liver. Eur Surg Res. 2007; 39(3):189–97. [PubMed: 17377393]

[31]. Yamada M, Burke C, Colditz P, Johnson DW, Gobe GC. Erythropoietin protects against apoptosis and increases expression of non-neuronal cell markers in the hypoxia-injured developing brain. J Pathol. May; 2011 224(1):101–9. [PubMed: 21404277]

[32]. Koh SH, Noh MY, Cho GW, Kim KS, Kim SH. Erythropoietin increases the motility of human bone marrow-multipotent stromal cells (hBM-MSCs) and enhances the production of neurotrophic factors from hBM-MSCs. Stem Cells Dev. Apr; 2009 18(3):411–21. [PubMed: 18590375]

[33]. Sandau KB, Faus HG, Brune B. Induction of hypoxia-inducible-factor 1 by nitric oxide is mediated via the PI 3K pathway. Biochem Biophys Res Commun. 2000; 278(1):263–7. [PubMed: 11071882]

[34]. Urao N, Okigaki M, Yamada H, et al. Erythropoietin-mobilized endothelial progenitors enhance reendothelialization via Akt-endothelial nitric oxide synthase activation and prevent neointimal hyperplasia. Circ Res. Jun 9; 2006 98(11):1405–13. [PubMed: 16645141]

[35]. Zhang D, Zhang F, Zhang Y, Gao X, Li C, Ma W, et al. Erythropoietin enhances the angiogenic potency of autologous bone marrow stromal cells in a rat model of myocardial infarction. Cardiology. 2007; 108(4):228–36. [PubMed: 17106196]

[36]. Kondyli M, Gatzounis G, Kyritsis A, Varakis J, Assimakopoulou M. Immunohistochemical detection of phosphorylated JAK-2 and STAT-5 proteins and correlation with erythropoietin receptor (EpoR) expression status in human brain tumors. J Neurooncol. Nov; 2010 100(2):157–64. [PubMed: 20336349]

[37]. Maiese K, Chong ZZ, Hou J, Shang YC. New strategies for Alzheimer's disease and cognitive impairment. Oxid Med Cell Longev. Nov-Dec; 2009 2(5):279–89. [PubMed: 20716915]

[38]. Dang J, Jia R, Tu Y, Xiao S, Ding G. Erythropoietin prevents reactive oxygen species generation and renal tubular cell apoptosis at high glucose level. Biomed Pharmacother. Dec; 2010 64(10): 681–5. [PubMed: 20685070]

[39]. Schlecht-Bauer D, Antier D, Machet MC, Hyvelin JM. Short- and Long-Term Cardioprotective Effect of Darbepoetin-alpha: Role of Bcl-2 Family Proteins. J Cardiovasc Pharmacol. Jul 10.2009

[40]. Bakker WJ, van Dijk TB, Parren-van Amelsvoort M, et al. Differential regulation of Foxo3a target genes in erythropoiesis. Mol Cell Biol. May; 2007 27(10):3839–54. [PubMed: 17353275]

[41]. Maiese K, Chong ZZ, Hou J, Shang YC. The "O" class: crafting clinical care with FoxO transcription factors. Adv Exp Med Biol. 2009; 665:242–60. [PubMed: 20429429]

[42]. Maiese K, Chong ZZ, Shang YC. "Sly as a FOXO": New paths with Forkhead signaling in the brain. Curr Neurovasc Res. Nov; 2007 4(4):295–302. [PubMed: 18045156]

[43]. Maiese K, Chong ZZ, Shang YC. OutFOXOing disease and disability: the therapeutic potential of targeting FoxO proteins. Trends Mol Med. May; 2008 14(5):219–27. [PubMed: 18403263]

[44]. Maiese K, Chong ZZ, Shang YC, Hou J. FoxO proteins: cunning concepts and considerations for the cardiovascular system. Clin Sci (Lond). Feb; 2009 116(3):191–203. [PubMed: 19118491]

[45]. Balan V, Miller GS, Kaplun L, et al. Life span extension and neuronal cell protection by Drosophila nicotinamidase. J Biol Chem. Oct 10; 2008 283(41):27810–9. [PubMed: 18678867]

[46]. Chong ZZ, Lin SH, Li F, Maiese K. The sirtuin inhibitor nicotinamide enhances neuronal cell survival during acute anoxic injury through Akt, Bad, PARP, and mitochondrial associated "anti-apoptotic" pathways. Curr Neurovasc Res. Oct; 2005 2(4):271–85. [PubMed: 16181120]

[47]. Chong ZZ, Maiese K. Enhanced Tolerance against Early and Late Apoptotic Oxidative Stress in Mammalian Neurons through Nicotinamidase and Sirtuin Mediated Pathways. Curr Neurovasc Res. Aug; 2008 5(3):159–70. [PubMed: 18691073]

[48]. Hisahara S, Chiba S, Matsumoto H, et al. Histone deacetylase SIRT1 modulates neuronal differentiation by its nuclear translocation. Proc Natl Acad Sci USA. Oct 7; 2008 105(40): 15599–604. [PubMed: 18829436]

[49]. Maiese K, Chong ZZ, Hou J, Shang YC. The vitamin nicotinamide: translating nutrition into clinical care. Molecules. 2009; 14(9):3446–85. [PubMed: 19783937]

[50]. Orimo M, Minamino T, Miyauchi H, et al. Protective role of SIRT1 in diabetic vascular dysfunction. Arterioscler Thromb Vasc Biol. Jun; 2009 29(6):889–94. [PubMed: 19286634]

[51]. Hasegawa K, Wakino S, Yoshioka K, et al. Sirt1 protects against oxidative stress-induced renal tubular cell apoptosis by the bidirectional regulation of catalase expression. Biochem Biophys Res Commun. Jul 18; 2008 372(1):51–6. [PubMed: 18485895]

[52]. Hou J, Chong ZZ, Shang YC, Maiese K. Early apoptotic vascular signaling is determined by Sirt1 through nuclear shuttling, forkhead trafficking, bad, and mitochondrial caspase activation. Curr Neurovasc Res. May; 2010 7(2):95–112. [PubMed: 20370652]

[53]. Chong ZZ, Kang JQ, Maiese K. AKT1 drives endothelial cell membrane asymmetry and microglial activation through Bcl-xL and caspase 1, 3, and 9. Exp Cell Res. Jun 10; 2004 296(2): 196–207. [PubMed: 15149850]

[54]. Hou J, Chong ZZ, Shang YC, Maiese K. FoxO3a governs early and late apoptotic endothelial programs during elevated glucose through mitochondrial and caspase signaling. Mol Cell Endocrinol. Mar 4; 2010 321(2):194–206. [PubMed: 20211690]

[55]. Abbott NJ, Hughes CC, Revest PA, Greenwood J. Development and characterisation of a rat brain capillary endothelial culture: towards an in vitro blood-brain barrier. J Cell Sci. Sep; 1992 103(Pt 1):23–37. [PubMed: 1429907]

[56]. Shang YC, Chong ZZ, Hou J, Maiese K. FoxO3a governs early microglial proliferation and employs mitochondrial depolarization with caspase 3, 8, and 9 cleavage during oxidant induced apoptosis. Curr Neurovasc Res. Nov; 2009 6(4):223–38. [PubMed: 19807657]

[57]. Shang YC, Chong ZZ, Hou J, Maiese K. Wnt1, FoxO3a, and NF-kappaB oversee microglial integrity and activation during oxidant stress. Cell Signal. Sep; 2010 22(9):1317–29. [PubMed: 20462515]

[58]. Kang JQ, Chong ZZ, Maiese K. Critical role for Akt1 in the modulation of apoptotic phosphatidylserine exposure and microglial activation. Mol Pharmacol. Sep; 2003 64(3):557–69. [PubMed: 12920191]

[59]. Kang JQ, Chong ZZ, Maiese K. Akt1 protects against inflammatory microglial activation through maintenance of membrane asymmetry and modulation of cysteine protease activity. J Neurosci Res. Oct 1; 2003 74(1):37–51. [PubMed: 13130504]

[60]. Chong ZZ, Lin SH, Maiese K. Nicotinamide Modulates Mitochondrial Membrane Potential and Cysteine Protease Activity during Cerebral Vascular Endothelial Cell Injury. J Vasc Res. 2002; 39(2):131–47. [PubMed: 12011585]

[61]. Chong ZZ, Lin SH, Maiese K. The NAD+ precursor nicotinamide governs neuronal survival during oxidative stress through protein kinase B coupled to FOXO3a and mitochondrial membrane potential. J Cereb Blood Flow Metab. Jul; 2004 24(7):728–43. [PubMed: 15241181]

[62]. Shang YC, Chong ZZ, Hou J, Maiese K. The forkhead transcription factor FoxO3a controls microglial inflammatory activation and eventual apoptotic injury through caspase 3. Curr Neurovasc Res. Feb; 2009 6(1):20–31. [PubMed: 19355923]

[63]. Solomon JM, Pasupuleti R, Xu L, et al. Inhibition of SIRT1 catalytic activity increases p53 acetylation but does not alter cell survival following DNA damage. Mol Cell Biol. Jan; 2006 26(1):28–38. [PubMed: 16354677]

[64]. Tanno M, Sakamoto J, Miura T, Shimamoto K, Horio Y. Nucleocytoplasmic shuttling of the NAD+-dependent histone deacetylase SIRT1. J Biol Chem. Mar 2; 2007 282(9):6823–32. [PubMed: 17197703]

[65]. Maiese K, Chong ZZ, Shang YC, Hou J. A “FOXO” in sight: targeting Foxo proteins from conception to cancer. Med Res Rev. May; 2009 29(3):395–418. [PubMed: 18985696]

[66]. Zhu W, Bijur GN, Styles NA, Li X. Regulation of FOXO3a by brain-derived neurotrophic factor in differentiated human SH-SY5Y neuroblastoma cells. Brain Res Mol Brain Res. Jul 5; 2004 126(1):45–56. [PubMed: 15207915]

[67]. Chong ZZ, Li F, Maiese K. Oxidative stress in the brain: Novel cellular targets that govern survival during neurodegenerative disease. Prog Neurobiol. Feb; 2005 75(3):207–46. [PubMed: 15882775]

[68]. Morissette M, Al Sweidi S, Callier S, Di Paolo T. Estrogen and SERM neuroprotection in animal models of Parkinson's disease. Mol Cell Endocrinol. Aug 13; 2008 290(1-2):60–9. [PubMed: 18515001]

[69]. Chong ZZ, Li F, Maiese K. Stress in the brain: novel cellular mechanisms of injury linked to Alzheimer's disease. Brain Res Brain Res Rev. Jul; 2005 49(1):1–21. [PubMed: 15960984]

[70]. Chong ZZ, Li F, Maiese K. Employing new cellular therapeutic targets for Alzheimer's disease: a change for the better? Curr Neurovasc Res. Jan; 2005 2(1):55–72. [PubMed: 16181100]

[71]. Hao J, Shen W, Tian C, et al. Mitochondrial nutrients improve immune dysfunction in the type 2 diabetic Goto-Kakizaki rats. J Cell Mol Med. Apr; 2009 13(4):701–11. [PubMed: 18410524]

[72]. Leuner K, Hauptmann S, Abdel-Kader R, et al. Mitochondrial dysfunction: the first domino in brain aging and Alzheimer's disease? Antioxid Redox Signal. Oct; 2007 9(10):1659–75. [PubMed: 17867931]

[73]. Li F, Chong ZZ, Maiese K. Microglial integrity is maintained by erythropoietin through integration of Akt and its substrates of glycogen synthase kinase-3beta, beta-catenin, and nuclear factor-kappaB. Curr Neurovasc Res. Aug; 2006 3(3):187–201. [PubMed: 16918383]

[74]. Mason-Garcia M, Beckman BS, Brookins JW, et al. Development of a new radioimmunoassay for erythropoietin using recombinant erythropoietin. Kidney Int. Nov; 1990 38(5):969–75. [PubMed: 2266682]

[75]. Namiuchi S, Kagaya Y, Ohta J, et al. High serum erythropoietin level is associated with smaller infarct size in patients with acute myocardial infarction who undergo successful primary percutaneous coronary intervention. J Am Coll Cardiol. May 3; 2005 45(9):1406–12. [PubMed: 15862410]

[76]. Bierer R, Peceny MC, Hartenberger CH, Ohls RK. Erythropoietin concentrations and neurodevelopmental outcome in preterm infants. Pediatrics. Sep; 2006 118(3):e635–40. [PubMed: 16908620]

[77]. Sohmiya M, Kakiba T, Kato Y. Therapeutic use of continuous subcutaneous infusion of recombinant human erythropoietin in malnourished predialysis anemic patients with diabetic nephropathy. Eur J Endocrinol. Oct; 1998 139(4):367–70. [PubMed: 9820611]

[78]. Ponikowski P, Jankowska EA. EPO's rescue mission in acute myocardial infarction: still more hopes than evidence. Eur Heart J. Nov; 2010 31(21):2577–9. [PubMed: 20802249]

[79]. Taniguchi N, Nakamura T, Sawada T, et al. Erythropoietin prevention trial of coronary restenosis and cardiac remodeling after ST-elevated acute myocardial infarction (EPOC-AMI): a pilot, randomized, placebo-controlled study. Circ J. Oct 25; 2010 74(11):2365–71. [PubMed: 20834185]

[80]. Soares MM, King SW, Thorpe PE. Targeting inside-out phosphatidylserine as a therapeutic strategy for viral diseases. Nat Med. Dec; 2008 14(12):1357–62. [PubMed: 19029986]

[81]. Chong ZZ, Kang J, Li F, Maiese K. mGluRI Targets Microglial Activation and Selectively Prevents Neuronal Cell Engulfment Through Akt and Caspase Dependent Pathways. Curr Neurovasc Res. Jul; 2005 2(3):197–211. [PubMed: 16181114]

[82]. Jessel R, Haertel S, Socaciu C, Tykhonova S, Diehl HA. Kinetics of apoptotic markers in exogeneously induced apoptosis of EL4 cells. J Cell Mol Med. 2002; 6(1):82–92. [PubMed: 12003671]

[83]. Mallat M, Marin-Teva JL, Cheret C. Phagocytosis in the developing CNS: more than clearing the corpses. Curr Opin Neurobiol. Feb; 2005 15(1):101–7. [PubMed: 15721751]

[84]. Zhang QJ, Wang Z, Chen HZ, et al. Endothelium-specific overexpression of class III deacetylase SIRT1 decreases atherosclerosis in apolipoprotein E-deficient mice. Cardiovasc Res. Nov 1; 2008 80(2):191–9. [PubMed: 18689793]

[85]. Ungvari Z, Labinskyy N, Mukhopadhyay, et al. Resveratrol attenuates mitochondrial oxidative stress in coronary arterial endothelial cells. Am J Physiol Heart Circ Physiol. Nov; 2009 297(5):H1876–81. [PubMed: 19749157]

[86]. Li F, Chong ZZ, Maiese K. Cell Life Versus Cell Longevity: The Mysteries Surrounding the NAD(+) Precursor Nicotinamide. Curr Med Chem. 2006; 13(8):883–95. [PubMed: 16611073]

[87]. Ni YG, Wang N, Cao DJ, et al. FoxO transcription factors activate Akt and attenuate insulin signaling in heart by inhibiting protein phosphatases. Proc Natl Acad Sci USA. Dec 18; 2007 104(51):20517–22. [PubMed: 18077353]

[88]. Maiese K, Chong ZZ, Shang YC, Hou J. Clever cancer strategies with FoxO transcription factors. Cell Cycle. Dec 15; 2008 7(24):3829–39. [PubMed: 19066462]

[89]. Astiz M, de Alaniz MJ, Marra CA. Effect of pesticides on cell survival in liver and brain rat tissues. Ecotoxicol Environ Saf. Oct; 2009 72(7):2025–32. [PubMed: 19493570]

[90]. Campos-Esparza MR, Sanchez-Gomez MV, Matute C. Molecular mechanisms of neuroprotection by two natural antioxidant polyphenols. Cell Calcium. Apr; 2009 45(4):358–68. [PubMed: 19201465]

[91]. Maiese K, Hou J, Chong ZZ, Shang YC. A fork in the path: Developing therapeutic inroads with FoxO proteins. Oxid Med Cell Longev. Jul; 2009 2(3):119–29. [PubMed: 20592766]

[92]. Maiese K, Li F, Chong ZZ, Shang YC. The Wnt signaling pathway: Aging gracefully as a protectionist? Pharmacol Ther. Apr; 2008 118(1):58–81. [PubMed: 18313758]

[93]. Takayama K, Ishida K, Matsushita T, et al. SIRT1 regulation of apoptosis of human chondrocytes. Arthritis Rheum. Sep; 2009 60(9):2731–40. [PubMed: 19714620]

[94]. Anekonda TS, Adamus G. Resveratrol prevents antibody-induced apoptotic death of retinal cells through upregulation of Sirt1 and Ku70. BMC Res Notes. 2008; 1:122. [PubMed: 19046449]

[95]. Okutan O, Solaroglu I, Beskonakli E, Taskin Y. Recombinant human erythropoietin decreases myeloperoxidase and caspase-3 activity and improves early functional results after spinal cord injury in rats. J Clin Neurosci. Apr; 2007 14(4):364–8. [PubMed: 17236773]

[96]. Wang ZY, Shen LJ, Tu L, et al. Erythropoietin protects retinal pigment epithelial cells from oxidative damage. Free Radic Biol Med. Apr 15; 2009 46(8):1032–41. [PubMed: 19136057]

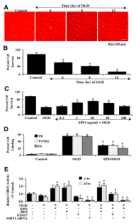

Fig. (1). EPO increases SIRT1 activity and prevents EC injury during OGD

(**A**) Primary cerebral ECs were exposed to OGD for 6, 8 and 12 hours and EC survival was determined 24 hours after OGD. Representative images illustrate that OGD leads to progressively increased EC injury over time. Control = untreated EC. (**B**) Quantitative analysis shows that EC survival was significantly decreased to 57 ± 6% (6 h), 39 ± 4% (8 h), and 12 ± 4% (12 h) after OGD when compared to untreated control cultures (97 ± 8%, **P*<0.01 *vs*. control). Each data point represents the mean and SEM from 6 experiments. (**C**) A range of EPO dosage (0.1, 1, 10, 50 and 100 ng/ml) was applied 1 h prior to a 8 hour period of OGD, EPO (1-50 ng/ml) significantly reduced trypan blue uptake and increased survival during OGD. The concentration of EPO (10 ng/ml) provides the maximal EC survival. Concentrations lower than 0.1 ng/ml or higher than 50 ng/ml did not improve EC survival during OGD. (**D**) A significant increase in the staining of trypan blue (TB, 55 ± 4%), apoptotic DNA fragmentation (TUNEL, 55 ± 3 %), phosphatidylserine (PS, 54 ± 6%) exposure 24 hours after a 8 hour period of OGD. In contrast, EPO (10 ng/ml) application significantly reduced cell labeling to 28 ± 1% (TB), 28 ± 2 % (TUNEL), and 20 ± 5% (PS) (**P*<0.01 *vs*. OGD). Each data point represents the mean and SEM from 6 experiments. (**E**) EPO (10 ng/ml), resveratrol (RES 15 μM), EX527 (2 μM) 1 hour pretreatment and SIRT1 siRNA transfection were assessed with their ability to alter SIRT1 HDAC activity at 6 hours and 24 hours after OGD. HDAC activity in ECs significantly decreased at 24 hours after OGD (**P*<0.05 *vs*. untreated ECs = Control). EPO, RES, or EPO/RES significantly increased HDAC in ECs, while EX527 and SIRT1 siRNA decreased HDAC activity (†*P* <0.05 *vs*. OGD). Each data point represents the mean and SEM from 6 experiments.

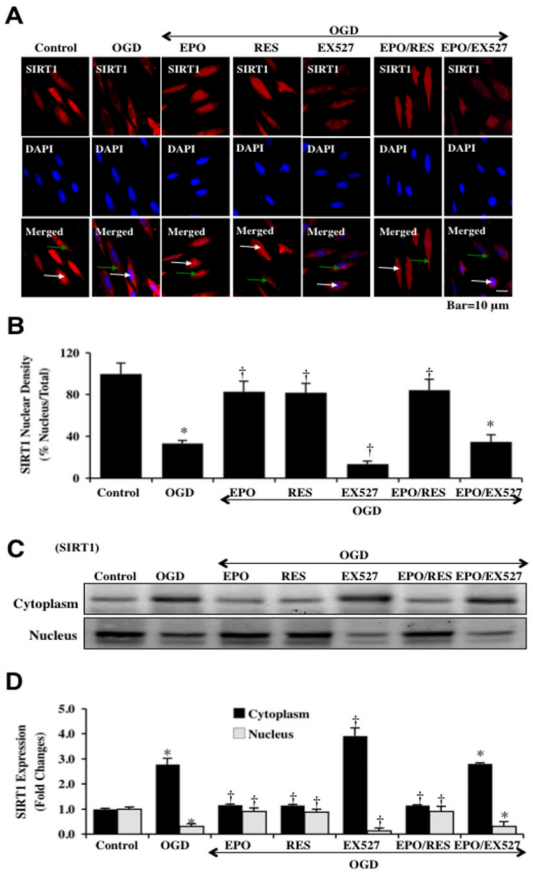

Fig. (2). EPO preserves SIRT1 nuclear shuttling in ECs during OGD

(**A**) ECs were imaged at 6 hours after OGD with immunofluorescent staining for SIRT1 (Texas-red streptavidin). Nuclei of ECs were counterstained with DAPI. In merged images, untreated control ECs do not have visible nuclei (red in color, white arrows) that illustrate nuclear localization of SIRT1. However, merged images after OGD show ECs with distinctly blue nuclei and red cytoplasm (green arrows) illustrating that SIRT1 is confined to the cytoplasm. In addition, inhibition of SIRT1 catalytic activity with EX527 (2 μM) also confined SIRT1 to the cytoplasm to a greater degree than OGD alone. Yet, EPO (10 ng/ml), resveratrol (RES 15 μM) or EPO/RES during OGD maintained SIRT1 in the nucleus of ECs (**P*<0.01 *vs*. untreated ECs = Control; †*P* <0.01 *vs*. OGD). **(B**) Quantification of the intensity of SIRT1 nuclear staining was performed using the public domain NIH Image program (http://rsb.info.nih.gov/nih-image). Each data point represents the mean and SEM from 6 experiments. (**C**) Equal amounts of cytoplasmic or nuclear protein extracts (50 μg/lane) were immunoblotted with anti-SIRT1 at 6 hours after OGD. SIRT1 expression is confined to the cytoplasm after OGD, but EPO (10 ng/ml), resveratrol (RES 15 μM), or EPO/RES application leads to the translocation of endogenous SIRT1 from the cytoplasm to the nucleus. SIRT1 inhibitor EX527 (2 μM) prevents the translocation of SIRT1 to the nucleus to a greater level than OGD alone. **(D**) Quantification of band density of SIRT1 was performed using the public domain NIH Image program (http://rsb.info.nih.gov/nih-image). (**P*<0.01 *vs*. untreated ECs = Control; †*P* <0.01 *vs*. OGD). Each data point represents the mean and SEM from 6 experiments.

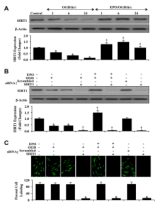

Fig. (3). EPO increases the expression of SIRT1 in ECs during OGD

(**A**) EC protein extracts (50 μg/lane) were immunoblotted with anti-SIRT1 (SIRT1) at 1, 6 and 24 hours after OGD. SIRT1 expression is progressively reduced over 24 hours after OGD exposure (**P*<0.01 *vs*. control), EPO (10 ng/ml) significantly increased SIRT1 expression at 1, 6 and 24 hours compared with OGD alone (†*P* <0.01 *vs*. OGD). (**B**) EC protein extracts (50 μg/lane) were immunoblotted with anti-SIRT1 (SIRT1) at 6 hours after OGD, gene knockdown of *SIRT1* siRNA significantly reduced expression of SIRT1. Non-specific scrambled siRNA did not significantly alter SIRT1 (**P*<0.01 *vs*. untreated ECs = Control; †*P* <0.01 *vs*. OGD). Quantification of the western band intensity was performed using the public domain NIH Image program (http://rsb.info.nih.gov/nih-image). (**C**) Transfection of siRNA against SIRT1 was performed in ECs and the expression of SIRT1 protein was assessed by immunofluorescence. In ECs with *SIRT1* gene knockdown, no significant expression of SIRT1 protein is present (**P*<0.01 *vs*. untreated ECs = Control or OGD).

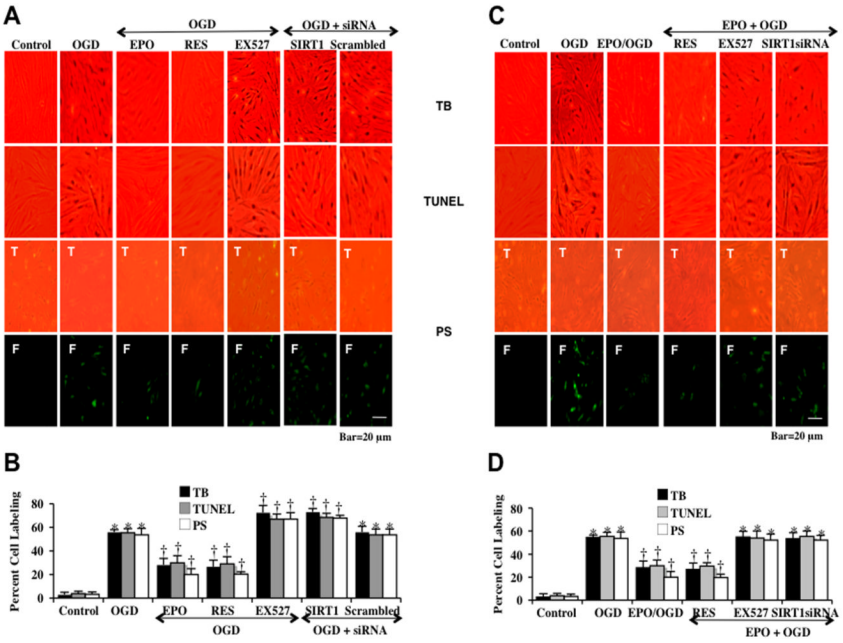

Fig. (4). EPO protects against EC injury through blocking apoptotic early phosphatidylserine (PS) exposure and nuclear DNA degradation in ECs during OGD

(A and **C)** Representative images demonstrate that OGD led to a significant increase in percent trypan blue staining, DNA fragmentation, and membrane PS exposure in ECs at 24 hours after OGD compared to untreated control cultures, which was prevented by EPO (10 ng/ml), resveratrol (RES 15 μM) or EPO/RES combined application. Yet, inhibition of SIRT1 activity with EX527 (2 μM) or gene silence of *SIRT1* with siRNA significantly increased apoptotic injury to a greater level during OGD and attenuated the efficacy of EPO. **(B** and **D)** Quantification of these results illustrate that EPO (10 ng/ml) application significant decreased percent trypan blue uptake, DNA fragmentation, and membrane PS exposure 24 hours after OGD when compared to OGD treated alone (**P* < 0.01 *vs*. untreated control; †*P* <0.05 *vs*. OGD). Inhibition of SIRT1 activity with EX527 (2 μM) or gene silence of *SIRT1* with siRNA significantly increased apoptotic injury to a greater level beyond OGD alone and attenuated the efficacy of EPO. Each data point represents the mean and SEM from 6 experiments.

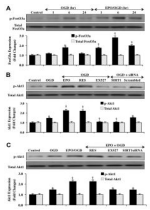

Fig. (5). EPO increases the expression of SIRT1, phosphorylated FoxO3a and Akt1 in ECs during OGD

(**A**) Primary EC protein extracts (50 μg/lane) were immunoblotted with anti-phosphorylated-FoxO3a (p-FoxO3a, Ser^{253}) or anti-total FoxO3a at 1, 6 and 24 hours after OGD. The expression of phospho-FoxO3a (p-FoxO3a) is initially increased at 6 hours but then lost at 24 hours after OGD (**P*<0.01 *vs*. control). EPO (10 ng/ml) one hour pretreatment significantly increased p-FoxO3a expression at 1, 6 and 24 hours compared with OGD alone (†*P* <0.01 *vs*. OGD). Quantification of western band intensity was performed using the public domain NIH Image program (http://rsb.info.nih.gov/nih-image). (**B** and **C**) Primary EC protein extracts (50 μg/lane) were immunoblotted with anti-phosphorylated-Akt1 (p-Akt1, Ser^{473}) or anti-total Akt1 at 6 hours after OGD. The expression of p-Akt1 (active) was mild increased at 6 hours compared with control (**P*<0.01 *vs*. control) and was further increased by application of EPO (10 ng/ml), resveratrol (RES 15 μM), or EPO/RES (†*P* <0.01 *vs*. OGD). Inhibition of SIRT1 activity with EX527 (2 μM) or gene silence of *SIRT1* with siRNA abolished the effect of EPO on p-Akt1 expression during OGD (†*P* <0.01 *vs*. OGD). Transfection with non-specific scrambled siRNA did not alter the expression of phosphorylated Akt1. Quantification of western band intensity was performed using the public domain NIH Image program (http://rsb.info.nih.gov/nih-image).

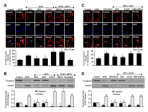

Fig. (6). EPO controls subcellular trafficking of FoxO3a and retains FoxO3a in the cytoplasm of ECs during OGD

(A and **C)** ECs were imaged 6 hours after OGD with immunofluorescent staining for FoxO3a (Texas-red streptavidin). Nuclei of ECs were counterstained with DAPI. In merged images, untreated control ECs have visible nuclei (dark blue in color, white arrows) that illustrate absence of FoxO3a in the nucleus and OGD exposure ECs were revealed with completely red cytoplasm (green arrows) and no visible nucleus with DAPI illustrating translocation of FoxO3a to the nucleus. Application of EPO (10 ng/ml), resveratrol (RES 15 μM), or EPO/RES maintains the expression of FoxO3a in the cytoplasm of ECs. However, inhibition of SIRT1 catalytic activity with EX527 (2 μM) or gene silence of *SIRT1* with transfection of SIRT1 siRNA (siRNA) during OGD results in significant nuclear translocation of FoxO3a during OGD (**P*<0.01 *vs*. untreated ECs = Control; †*P* <0.01 *vs*. OGD). Quantification of the intensity of FoxO3a nuclear staining was performed using the public domain NIH Image program (http://rsb.info.nih.gov/nih-image). Each data point represents the mean and SEM from 6 experiments. (**B** and **D)** Equal amounts of cytoplasmic (cytoplasm) or nuclear (nucleus) protein extracts (50 μg/lane) were immunoblotted with anti-FoxO3a at 6 hours after OGD. OGD alone or with the inhibitor of SIRT1 EX527 (2 μM) or transfection with *SIRT1* siRNA during OGD induced significant nuclear translocation of FoxO3a. In contrast, EPO (10 ng/ml), resveratrol (RES 15 μM) or EPO/RES retained FoxO3a protein in the cytoplasm during OGD (**P*<0.01 *vs*. untreated ECs = Control; †*P* <0.01 *vs*. OGD).

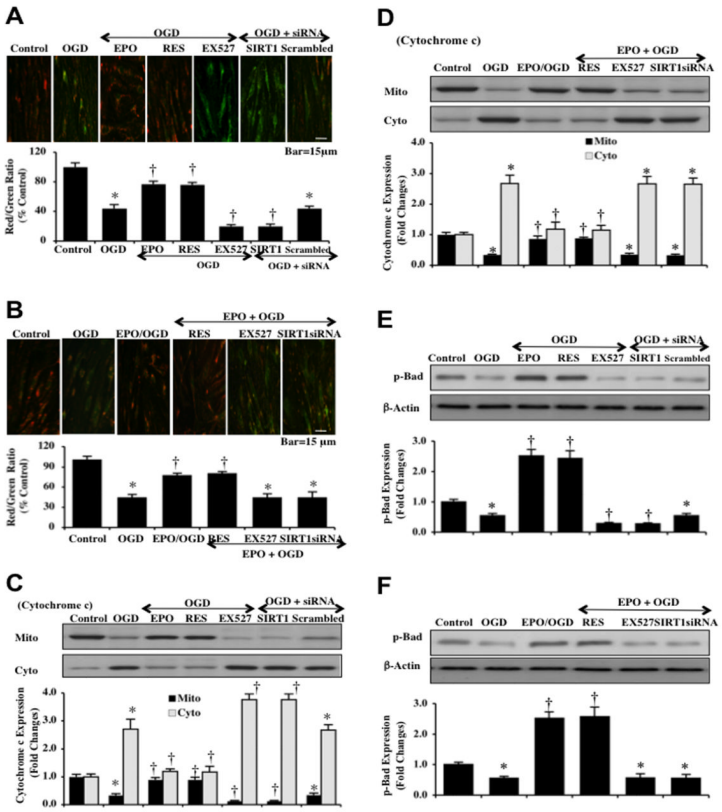

Fig. (7). EPO inhibits mitochondrial depolarization, cytochrome c release, and Bad activation through SIRT1 during OGD

(**A** and **B)** OGD induces a significant decrease in the red/green fluorescence intensity ratio of mitochondria using the cationic membrane potential indicator JC-1 at 6 hours when compared with untreated control ECs. EPO (10 ng/ml), resveratrol (RES 15 μM), or EPO/RES combined treatment during OGD significantly increased the red/green fluorescence intensity of mitochondria in ECs, demonstrating that mitochondrial membrane potential was restored. In contrast, inhibition of SIRT1 with EX527 (2 μM) and gene silence of *SIRT1* with transfection of SIRT1 siRNA (siRNA) worsened mitochondrial membrane depolarization to a greater degree than OGD alone. The relative ratio of red/green fluorescent intensity of mitochondrial staining was measured in 6 independent experiments with analysis performed using the public domain NIH Image program (http://rsb.info.nih.gov/nih-image) (untreated ECs = Control, **P*<0.01 *vs*. Control; †*P* <0.01 *vs*. OGD). (**C** and **D)** Equal amounts of mitochondrial (mito) or cytosol (cyto) protein extracts (50 μg/lane) were immunoblotted with cytochrome c demonstrating that EPO, RES, EPO/RES significantly prevented cytochrome c release from mitochondria 6 hours after OGD. SIRT1 inhibition (EX527, SIRT1 siRNA) and non-specific scrambled siRNA did not prevent cytochrome c release during OGD. Quantification of the western band intensity was performed using the public domain NIH Image program (http://rsb.info.nih.gov/nihimage) (untreated ECs = Control *vs*. OGD **P*<0.01 *vs*. Control; †*P* <0.01 *vs*. OGD). Each data point represents the mean and SEM from 6 experiments. (**E** and **F**) Primary EC protein extracts (50 μg/lane) were immunoblotted with anti-phosphorylated-Bad (p-Bad, Ser136) at 6 hours after OGD. Phosphorylated Bad (p-Bad) expression is promoted by EPO, RES, but is lost during inhibition of SIRT1 or *SIRT1* gene knockdown. Non-specific scrambled siRNA during OGD did not change Bad phosphorylation during OGD alone (untreated ECs = Control, **P*<0.01 *vs*. Control; †*P* <0.01 *vs*. OGD).

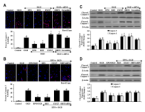

Fig. (8). EPO controls caspase 1 and caspase 3 activity during OGD

(**A** and **B)** ECs were exposed to OGD and caspase 3 activation was determined 6 hours after OGD through immunocytochemistry with antibody against cleaved active caspase 3 (17 kDa). Representative images illustrate active caspase 3 staining (red) in cells following OGD, but cellular red staining is almost absent in EPO (10 ng/ml) or resveratrol (RES 15 μM) pretreatment. Inhibition of SIRT1 activity with EX527 (2 μM) or gene knockdown of *SIRT1* significantly increased active caspase 3 expression to a greater degree in ECs that OGD alone, illustrating that SIRT1 activation was a robust modulator of caspase 3 activity. Non-specific scrambled siRNA did not eliminate caspase 3 activity during OGD. Quantification of caspase 3 immunocytochemistry was performed using the public domain NIH Image program (http://rsb.info.nih.gov/nih-image) (**P* <0.01 *vs*. untreated ECs = Control; †*P*<0.01 *vs*. OGD). (**C** and **D**) EC protein extracts (50 μg/lane) were immunoblotted with anti-cleaved caspase 3 antibody (active caspase 3, 17 kDa) and with anti-cleaved caspase 1 antibody (active caspase 1, 20 kDa) at 6 hours after OGD. OGD markedly increased cleaved caspase 3 and caspase 1 expression. Transfection with SIRT1 siRNA or inhibition of SIRT1 with EX527 (2 μM) results in a significant elevation in caspase 3 and caspase 1. EPO (10 ng/ml), resveratrol (RES, 15 μM), or EPO/RES combined treatment markedly reduced the expression of cleaved caspase 3 and caspase 1 during OGD. Quantification of western band intensity was performed using the public domain NIH Image program (http://rsb.info.nih.gov/nih-image) (**P* <0.01 *vs*. untreated ECs = Control; †*P*<0.01 *vs*. OGD).